INTERNATIONAL JOURNAL OF HYDROGEN ENERGY 34 (2009) 8193–8203

Available at www.sciencedirect.com

ScienceDirect

journal homepage: www.elsevier.com/locate/he

Catalytic activity vs. size correlation in platinum catalysts of PEM fuel cells prepared on carbon black by different methods

F.J. Nores-Pondal[a], I.M.J. Vilella[b], H. Troiani[c], M. Granada[a], S.R. de Miguel[b], O.A. Scelza[b], H.R. Corti[a,*]

[a]Departamento de Física de la Materia Condensada, Centro Atómico Constituyentes, Comisión Nacional de Energía Atómica (CNEA), General Paz 1499, 1650 San Martín, Buenos Aires, Argentina

[b]Instituto de Investigaciones en Catálisis y Petroquímica (INCAPE), Facultad de Ingeniería Química (Universidad Nacional del Litoral) – CONICET, Santiago del Estero 2654, 3000 Santa Fe, Argentina

[c]Departamento de Física, Centro Atómico Bariloche, Comisión Nacional de Energía Atómica (CNEA), Av. Bustillo 9500, 8400 San Carlos de Bariloche, Argentina

ARTICLE INFO

Article history:
Received 10 May 2009
Received in revised form
23 July 2009
Accepted 24 July 2009
Available online 12 August 2009

Keywords:
Pt catalysts
PEM fuel cell
Size effect
Vulcan XC-72
Dispersion

ABSTRACT

In this work nanoparticulated platinum catalysts have been prepared on carbon Vulcan XC-72 using three methods starting with chloroplatinic acid as a precursor: (i) formic acid as a reductor agent; (ii) impregnation method followed by reduction in hydrogen atmosphere at moderated temperature; and (iii) microwave-assisted reduction in ethylene glycol. The catalytic and size studies were also performed on a commercial Pt catalyst (E-Tek, De Nora).

The characterization of the particle size and distribution was performed by means of transmission electron microscopy (TEM) and X-ray diffraction (XRD). The characterizations of the catalytic and electrocatalytic properties of the catalysts were determined by studying the cyclohexane dehydrogenation reaction (CHD) and the behavior under cyclic voltammetry (CV) in sulfuric acid solutions. The measured electrochemical activity, along with the hydrogen chemisorption of the catalysts allows the estimation of effective particle sizes, which are much larger than those measured by TEM and XRD. The catalysts prepared by reduction with formic acid and ethylene glycol (microwave-assisted) show electrochemical activities very close to those of the commercial catalyst, and are almost insensitive to the Pt dispersion or Pt particle size. The chemical activity in CHD correlates well with the metallic dispersion determined by hydrogen chemisorption, indicating similar accesibility of H_2 and cyclohexane to the catalyst surface.

1. Introduction

Catalysts for proton exchange membrane fuel cells (PEMFC) are basically composed of platinum nanoparticles deposited on a carbon conducting support. The size and distributions of these nanoparticles influence the effectiveness of the hydrogen oxidation (HOR) and the oxygen reduction (ORR) reactions when these catalysts make a membrane electrode assembly (MEA) of the PEMFC [1–3].

* *Corresponding author*. Tel.: +54 11 6772 7174.
E-mail address: hrcorti@cnea.gov.ar (H.R. Corti).

0360-3199/$ – see front matter © 2009 Professor T. Nejat Veziroglu. Published by Elsevier Ltd. All rights reserved.
doi:10.1016/j.ijhydene.2009.07.073

Stevens and Dahn [4] indicate that the optimum size is around 2 nm for the HOR carried out on Vulcan-supported Pt catalysts, based on the measurement of the electrochemical surface area in acid solutions.

Several authors have studied the effect of the particle size of carbon-supported platinum particles on the ORR. Blurton et al. [5] showed that the electrocatalytic activity of platinum is 20 times lower on 1.5 nm crystallites than on crystalline platinum black, while Bett et al. [6] did not observed changes in the activity of carbon-supported platinum for particle sizes in the 3–40 nm range.

Kinoshita [7] pointed out some contradictory results about the effect of the platinum particle size on the ORR rate in acid solutions. While some authors indicated that the Pt-normalized mass activity (current per gram of Pt) seems to reach a maximum at about 3–5 nm [8,9], others observed that the mass activity increases as the Pt particle size decreases [6,10,11]. On the other hand, the specific activity (current normalized per cm^2 of Pt) decreases as the Pt particle size decreases according to some authors [8–10], while for others it is independent of the size [6,11,12]. The maximum in the mass activity found for particles around 3 nm by Kinoshita [7] was attributed to the change in the fraction of surface atoms on the (100) and (111) crystal faces of Pt particles and predicted that the specific activity should increase with an increasing Pt particle size. Perez et al. [12] showed that the specific activity for the ORR in acid media is mainly due to the (100) facets, while the (111) face is more active in alkaline electrolytes.

The Pt particle size effect on the ORR was recently reviewed by Gasteiger et al. [13]. They pointed out that the activities reported in the literature for pure Pt catalysts often vary by up to one order of magnitude and proposed to reproduce the PEMFC environment by performing thin-film rotating disc electrode (RDE) measurements on Pt catalysts in aqueous $HClO_4$. This study was performed with variable particle sizes, such as polycrystalline Pt (hundreds of nm), Pt-black (10–20 nm), and a Pt/C catalyst of very high specific area (120 $m^2\,g_{Pt}^{-1}$), with size ≈2 nm. The results confirmed the findings that no mass activity gains could be expected for catalysts with Pt surface areas exceeding 90 $m^2\,g_{Pt}^{-1}$ [14], corresponding to particle sizes of 3–4 nm. The size effect observed below this critical size was attributed to the potential-dependent adsorption of oxygenated intermediate species on the smaller particles, which hinder the rate-determining step of the ORR [14,15]. Antoine et al. [15] analyzed the ORR kinetics on Pt nanoparticles (2.5–28 nm) inside Nafion and found that a steep decrease of the specific activity for the smallest particles leads to a maximum mass activity for Pt particles of about 3 nm.

Yano et al. [16] studied the particle size effect on the ORR activity for Pt nanoparticles (1.6–4.8 nm) supported on carbon black, along with the ^{195}Pt NMR spectral features. They found that the electronic properties of the Pt surface atoms on nanoparticles do not exhibit any particle effect.

The size effect for the methanol oxidation reaction (MOR) with carbon-supported Pt nanoparticles has been also studied [17–19]. Thus, Takasu et al. [17] found that the specific activity for MOR on Pt catalyst with particle sizes between 2 and 6 nm decreases with a decrease in the particle size, while Park et al. [18] working with Pt particles with diameters in the range of 2–9 nm concluded that the specific activity decreases for nanoparticles smaller than 4 nm, but are similar to that observed on polycrystalline Pt for the larger particles. Bergamaski et al. [19] performed a detailed study of MOR with differential electrochemical mass spectrometry (DEMS) and concluded that the optimum particle size for the electrooxidation of methanol to CO_2 is between 3 and 10 nm. The loss of efficiency for particles smaller than 3 nm can be accounted by their morphology characteristics, whereas for particles larger than 10 nm the effect is related to weaker adsorption of the formaldehyde produced in the process.

Different reduction methods of the platinum precursor (usually chloroplatinic acid), which differ in the reduction agent employed, have been described in the literature, including the formic acid method [20,21], the impregnation method followed by reduction with hydrogen at high temperature [22] and the microwave-assisted method in ethylene glycol [23]. Dimethyl(1,5-cyclooctadiene) platinum(II) has been also used as a precursor in an impregnation method using supercritical carbon dioxide [24]. Alternative impregnation methods use $Pt(NH_3)_4(NO_3)_2$ [25], $Pt(NH_3)_4Cl_2$ or $Pt(NH_3)_4(OH)_2$ as precursors [26], followed by reduction with hydrogen at high temperature.

In the search for lower platinum loadings in PEMFC, different types of carbon supports have been analyzed as alternative to Vulcan, including pregraphitized carbon blacks [27], carbon nanotubes (CNT) [28,29] and graphite nanofibers [29,30], although Vulcan is nowadays the most extensively used support for Pt catalyst in PEM fuel cells.

In this work, the characteristic of supported Pt catalyst prepared on Vulcan by three different methods (formic acid, impregnation followed by reduction with hydrogen at moderate temperature, and microwave-assisted in ethylene glycol) is compared so as to correlate the size of the Pt particles with the electrocatalytic activity.

These liquid phase methods of platinum catalysts are more secure in what the experimental procedures it concerns and give particles sizes that are in the range of the ones obtained from more severe methods that involve, for example, the functionalization of the carbon surface with highly concentrated acids and at high temperatures.

2. Experimental

2.1. *Catalysts supports*

The carbon support used in this study is Vulcan XC-72 having a specific BET surface area of 250 $m^2\,g^{-1}$ and a mean particle size of 40 nm. The initial inorganic impurities present in Vulcan carbon were reduced, as summarized in Table 1, by successive treatments with aqueous solutions of 10 wt% HCl,

Table 1 – Impurities (wt%) of the carbon support before and after the purification treatment.

Support Impurities	Al	Si	S
Vulcan (before)	0.022	0.073	0.149
Vulcan (after)	0.006	0.012	0.025

HNO_3 and HF by 48 h each one. After drying at 120 °C, the material was thermally treated for 8 h at 850 °C under a hydrogen flow (5 mL g^{-1} min^{-1}) to eliminate sulphurated compounds, which could poison Pt particles.

2.2. Catalysts preparation

Catalysts containing 20 wt% Pt were prepared using three methods described below.

2.2.1. Formic acid method (FAM)

This method uses formic acid as a reduction agent and it consists of a three-step addition of 6.8 mL of 0.1 M H_2PtCl_6 aqueous solution (Aldrich, A.C.S. Reagent) to a stirring suspension made of 0.5 g of the carbon support in 25 mL of an aqueous solution of 0.1 M HCOOH (Merck, analytical grade) at 50 °C [20,21]. Each addition was done after the platinum was completely reduced, as indicated by the use of potassium iodide as an indicator. The reduction occurred preferentially on the surface of the carbon support and, when completed, the suspension was cooled down to room temperature and finally the catalyst was filtered and dried in air at 80 °C. We designed this catalyst as Pt/VF.

2.2.2. Wet impregnation method

The carbon support was added to a stirred solution (1400 rpm) of chloroplatinic acid, with a volume of solution/mass of support ratio of 30 mL g^{-1}, and the suspension was stirred for 4 h and finally heated to evaporation at 120 °C in order to ensure the complete deposition of the chloroplatinic acid on the support [22]. The reduction of the platinum was performed in a reactor at 100 °C, for 2 h under flowing hydrogen, which is a much less severe condition than the impregnation procedure previously used [22], carried out at 350 °C. The catalyst obtained by this method is designed as Pt/VI.

2.2.3. Microwave-assisted method

This method consisted of microwave heating of ethylene glycol solution of chloroplatinic acid, as described elsewhere [23]. Briefly, 1.0 mL of 0.05 M $H_2PtCl_6 \cdot 6H_2O$ (Aldrich, A.C.S. Reagent) aqueous solution was mixed with 25 mL of ethylene glycol (Carlo Erba), and 0.75 mL of 0.4 M KOH. Then, about 40 mg of Vulcan XC-72 carbon were added to the mixture and sonicated during 30 min. Finally, the mixture was heated in a household microwave oven (White Westinghouse, 800 W) for 50 s at the maximum power. The suspension was filtered and the residue was washed with acetone and dried at 100 °C over night in a vacuum oven. The catalyst obtained by this method is designed as Pt/VM.

2.3. Nanoparticle size characterization

The nanomorphology of supported catalysts was observed by transmission electron microscopy (TEM) using a Philips CM 200 apparatus. The samples for the TEM analysis were prepared by treating the catalyst powder in water for 1 h in an ultrasonic bath. A drop of the suspension was applied onto a clean 3 mm copper grid (mesh size 200) with carbon support film on it (Structure Probe, Inc.). The software Matrox Inspector, for image edition, was used to determine the particle size using TEM micrographs to build histograms of particle size distribution.

The catalyst samples were also analyzed by powder X-ray diffraction (XRD) techniques. The X-ray diffraction patterns were collected at ambient temperature on a Philips X'Pert System, using a PW-3710 controlled diffractometer, with sweep steps of 0.03° and counting time of 10 s, for 2θ ranging between 30° and 100°. In all cases the incident wavelength was 1.5406 Å (Cu Kα at 40 kV and 30 mA). The mean crystallite size of the catalyst was determined using Scherrer equation, based on the broadness of the peak associated to the (220) face of the face-centered cubic (f.c.c.) structure of platinum and assuming that the particles are spherical. The (220) peak of fcc platinum was chosen because it appears in a region where the carbon contributions can be neglected, allowing a Gaussian fitting of the peaks to eliminate the background contributions.

2.4. Hydrogen chemisorption

Hydrogen chemisorption measurements were carried out in discontinuous equipment. Samples were previously reduced at 100 °C for 3 h under flowing hydrogen, evacuated at 7×10^{-8} bar, and finally cooled down to room temperature. The hydrogen adsorption isotherms were performed at room temperature between 0.03 and 0.13 bar, and were lineal in this range of pressure.

The monolayer of hydrogen chemisorbed was calculated by extrapolation of the isotherm to pressure zero. From the data of chemisorbed H_2 the ratio between the moles of exposed Pt and the total moles of Pt (metallic dispersion) can be calculated considering the stoichiometry of chemisorbed H_2 on Pt (equal to 0.5 mol H_2/Pt atom).

2.5. Catalytic and electrocatalytic activities

Cyclohexane dehydrogenation reaction (CHD) was carried out in a differential flow reactor at 250 °C by using a H_2/cyclohexane molar ratio = 26. The reaction product was only benzene, and the reaction rate was determined by chromatographic analysis of the converted cyclohexane into benzene, using a FID as detector. The mass of catalyst used in the CHD experiments was chosen in such a way to obtain a conversion lower than 5% (differential reactor).

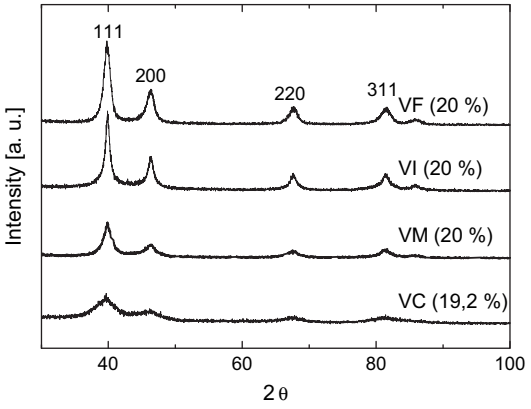

Fig. 1 – X-ray diffractograms of platinum catalysts prepared using different methods. $\lambda = 1.54056$ Å (Cu Kα).

Table 2 – Average particle sizes (*d*) of the Pt catalysts determined by TEM and XRD and comparison with the results in the literature.

Catalysts	Support	Method	Pt load (%)	*d* (TEM) (nm)	*d* (XRD) (nm)	Reference
Pt/VC	V	E-TEK	19.2	2.2	2.7	This work
	V		20	2.8	2.8	[12]
	V		20	–	3.7	[34]
	V		20	–	4.0	[33]
	V		20	2.8	–	[36]
	V		20	2.9	–	[1]
	V		20	2.5	–	[35]
	V		20	3.4	–	[37]
	CB		20	1.2	–	[36]
Pt/VM	V	MWEG	20	5.3	5.4	This work
	V		18.9	3.8 ± 0.3	–	[23]
	CNT		19.4	3.6 ± 0.3	–	[23]
Pt/VF	V	FA	20	7.3	6.5	This work
	V		17–20	–	2.5–4.4	[20]
	V		23–28	–	3.7–5.0	[20]
	CB		10	–	8.4	[41]
Pt/VI	V	I	20	3.2	7.5	This work
	V	I	10	2.0	–	[25]
	CNF	I	3.4	1.4–1.5	–	[25]
	V	I	5.0	1.75	–	[26]
	V	I	8.1	2	–	[26]
	HCS	IwH_2	9.3	–	5.3	[34]
	V	F	25	–	10.2	[39]
	V[a]		25	–	4.8	[39]
	V[b]		25	–	9.4	[39]
	CNT	EG	10	2.6	–	[28]
	HCS		9.6	–	4.7	[34]
	MCMB		6.5	–	4.6	[34]
	CC		20	2.7	–	[42]
	V	EGF	40	7.1	–	[43]
	CA	SCD	20–37	2	–	[40]
	CB	R	15	1.5	–	[44]
	GP	IE	6.2	1.2	–	[32]
	CB	C	10	–	6.3–8.4	[41]
	CB	C[c]	10	–	4.2–5.3	[41]

Carbon supports: CA – carbon aerogel; CB – carbon black; CC – carbon cryogel; CNF – carbon nanofibers; CNT – carbon nanotubes; GP – graphite powder; HCS – hard carbon spherules; MCMB – mesocarbon microbeds; V – Vulcan. Method: C – colloidal; EG – ethylene glycol; EGF – ethylene glycol–formaldehyde; FA – formic acid; F – formaldehyde; I – impregnation with H_2; IE – ion exchange; IwH_2 – impregnation without reduction with H_2; MWEG – microwave-assisted ethylene glycol; R – radiolytic; SCD – supercritical CO_2.

a Preoxidated Vulcan.

b Postoxidated Vulcan.

c Reduced with $NaBH_4$ or sodium formate.

The electrochemical characterization of the catalysts was performed with the cyclic voltammetry technique using a potentiostat/galvanostat (TEQ-02, Argentina) with a conventional three-electrode cell. The working electrode consisted in an active layer made with a suspension blended from 60 mg of Pt/C, 0.5 mL of 5 wt% Nafion™ solution in alcohol (Ion Power Inc.), and 0.5 mL of deionized water. After homogenization in an ultrasonic bath (1 h), 8 μL of this suspension was deposited on a glassy carbon electrode (area 0.2 cm^2) previously polished with alumina paste (Micropolish) up to 1 μm, and washed for 15 min in three successive solutions (previously submitted to a ultrasonic treatment) of acetone, ethanol–water (1:1), and water, respectively. The resulting layer (2.5 $mg_{Pt/C}\,cm^{-2}$) was dried in air for 1 h at 90 °C to ensure its binding to the glassy carbon rod. All experiments were carried out at room temperature (25 °C). The counter-electrode was a Pt foil and a saturated calomel electrode (SCE) was employed as a reference; all potentials are referred to its potential (+0.241 V versus normal hydrogen electrode, NHE). 1 M H_2SO_4 (Merck), degassed for 2 h with N_2 previous to each measurement, was used as electrolyte. The inert gas stream was held above the solution and then 10 voltametric cycles at 50 $mV\,s^{-1}$ (−0.191 to +1.159 V vs. SCE) were applied to clean the catalyst surface. Two voltammograms were then monitored in the potential range of −0191 to 0.259 V vs. SCE at the same sweeping rate. The electrochemical active area of Pt was

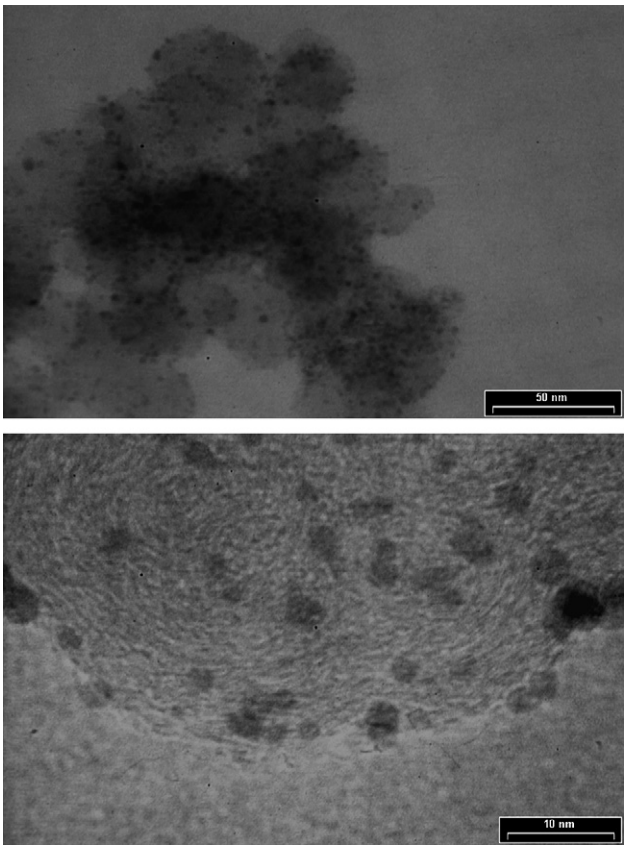

Fig. 2 – TEM micrographs (at different magnifications) of commercial 19.2% Pt Vulcan catalysts (E-TEK).

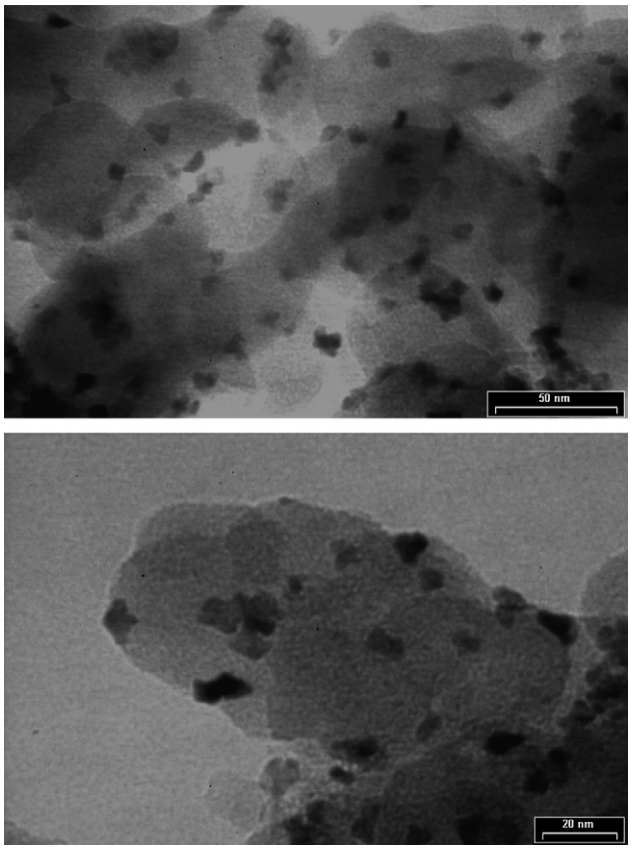

Fig. 3 – TEM micrographs (at different magnifications) of a Pt catalyst on Vulcan prepared by the formic acid method (Pt/VF).

determined from the integrated charge under the hydrogen adsorption peaks in the second cycle.

3. Results and discussion

3.1. *Pt particle size*

Fig. 1 shows the powder X-ray diffraction patterns for the prepared catalysts. In all cases, the peaks observed indicate the presence of the face-centered cubic (fcc) structure typical of platinum metal, represented by the planes (111), (200), (220), and (311). The broader diffractions peaks for VC and VM are an indication of small average particle size as expected from Scherrer equation. The broadening in the peaks is also an evidence for lower degree of crystallinity, typical of small particles having high lattice strain [31], although in the catalysts prepared in this study its contribution to broadening is minor. The calculated average size values follows the sequence Pt/VI > Pt/VF > Pt/VM > Pt/VC, as it can be seen in Table 2.

The TEM microphotographies show the size and distribution of Pt nanoparticles on the commercial catalysts (Fig. 2) and those prepared by the three methods (Figs. 3 and 4). The metal nanoparticles are homogeneously distributed on the Vulcan support in all the TEM micrographs analyzed, except for Pt/VI sample (Fig. 4a). Besides, the catalyst prepared by the impregnation method (Pt/VI) exhibits large particles, about 15 nm in size (see Fig. 4a), in addition to small particles, as observed for the commercial catalyst.

This behavior is reflected in the particle size distributions' histograms shown in Fig. 5a–d, obtained by directly measuring the size of 100 randomly chosen particles in the magnified TEM images.

The histogram of the particle size distribution for the commercial catalyst, shown in Fig. 5d, has the typical shape previously reported [1,34], although with a narrower size distribution (particles larger than 5 nm were absent). The Pt/VF catalyst histogram, Fig. 5a, shows a clear bimodal distribution with particle sizes ranging between 4 and 12 nm, with a certain contribution of the larger particles to the Pt exposed area.

The histograms of the Pt/VI and Pt/VM catalysts have a different profile than that observed for Pt/VF. The Pt/VI catalyst (Fig. 5b) seems to exhibit a bimodal distribution with small particle sizes (ca. 1.5 and 6 nm), similar to the pattern observed by Maillard et al. [31] for a Pt 5 wt% catalyst prepared by the ion exchange method on carbon black [32]. However, the main feature of this catalyst, as mentioned above, is the presence of large particles with sizes about 15 nm, which make an important contribution (ca. 25%) to the total Pt area.

Finally, the Pt/VM catalyst (Fig. 5c) exhibits a broader distribution, with particle sizes between 2 and 14 nm, with

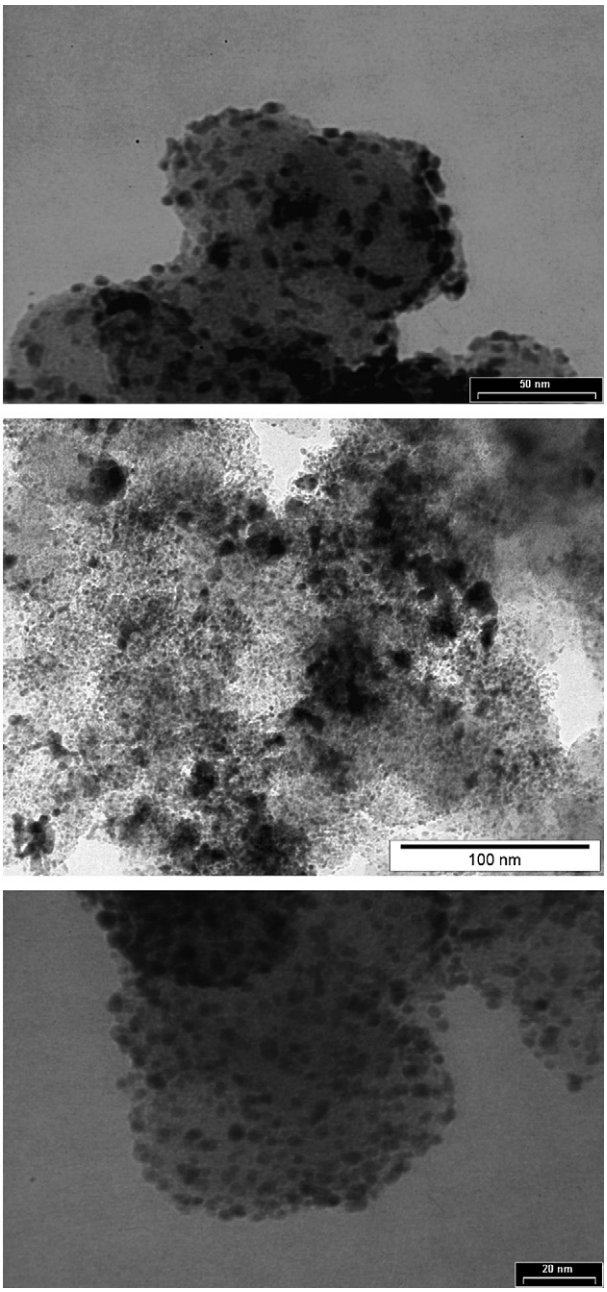

Fig. 4 – TEM micrographs (at different magnifications) of a Pt catalyst on Vulcan prepared by (a) the impregnation method (Pt/VI) and (b) the microwave-assisted method (Pt/VM).

particles larger than 9 nm representing an important contribution to the Pt exposed area. This histogram differs from that reported by Liu et al. [23], for Pt catalyst prepared by the microwave-assisted method with ethylene glycol on Vulcan and carbon nanotubes with Pt loadings close to 20 wt%, where a relatively narrow particle size distribution in the range 2–6 nm was found.

The average particle size was calculated from the histograms according to the following equation:

$$d = \frac{\sum_i f_i d_i}{\sum_i f_i} \quad (1)$$

where d is the average size of Pt particle, d_i is the mean diameter of the particles having diameters between $d_i - \Delta d \leq d_i \leq d_i + \Delta d$, and f_i is its corresponding frequency of occurrence. The sum extends over all the particles with $f_i \neq 0$ and $\Delta d = 0.75$ nm.

The average sizes of the Pt nanoparticles obtained by TEM for the catalysts prepared by different methods are summarized in Table 2, along with the values reported by other authors. It should be emphasized that, due to the heterogeneity of the sample, this average size is not always representative of the macroscopic average size, as obtained by the XRD technique, which scans the complete sample.

Some authors determined the average size of Pt particles using XRD and found values between 2.8 and 4 nm [12,33,34] for the E-TEK catalyst with 20 wt% Pt, as shown in Table 2. The average particle diameter of the same catalyst determined by TEM ranged from 2.5 to 3.4 nm [1,35–37]. The XRD and TEM average values of Pt particle size obtained in this work, reported in Table 2, are self consistent and close to the approximate value reported by the manufacturer (2.2 nm) [38] for this Pt loading.

The Pt particle average size determined by XRD for our catalysts (Pt 20 wt%) prepared on Vulcan by microwave-assisted method (Pt/VM) is similar to the average size determined by TEM, although larger (see Table 2) than that reported by Liu et al. [23] using TEM. This difference is clearly due to the contribution of particles larger than 6 nm observed in our catalyst (Fig. 5c).

The average size of the Pt particles in the catalyst prepared by reduction with formic acid (Pt/VF) determined by XRD is 7.9 nm, a value consistent with that measured by TEM, having in mind the bimodal distribution discussed above. This result agrees rather well with that reported for catalysts prepared with the same method on carbon black [41], while it is larger than that reported on Vulcan [20], probably because of differences in the surface state of the used supports. It is worthy to note that the Pt catalysts prepared with the formaldehyde method [39] exhibit particle size that, depending on the treatment of the support, are larger or smaller than that observed in the Pt/VF catalyst, as shown in Table 2.

The particle size determined by XRD for the Pt/VI catalyst prepared with the impregnation method (7.5 nm) is quite different to the TEM value (3.2 nm). The unusual profile of the size distribution (Fig. 5b), already discussed, is responsible for this difference because the larger particles seem to dominate the XRD average.

If we compare (see Table 2) the particle size of the catalyst with Pt 20 wt% determined by TEM with those reported by other authors on Vulcan using the same technique with lower Pt loadings [25,26], the expected behavior is observed, that is, the particle size decreases with the Pt loading. On the other hand, the particle size determined by XRD for the Pt/VI catalyst is more than double of the value obtained by TEM. Curiously, other study by XRD of a catalyst prepared by impregnation, although without the use of hydrogen as a reductor [34], leads to bigger particle size than the catalyst studied by TEM at similar Pt loading, and correlates quite well with that measured in this work, having into account the difference in Pt loading.

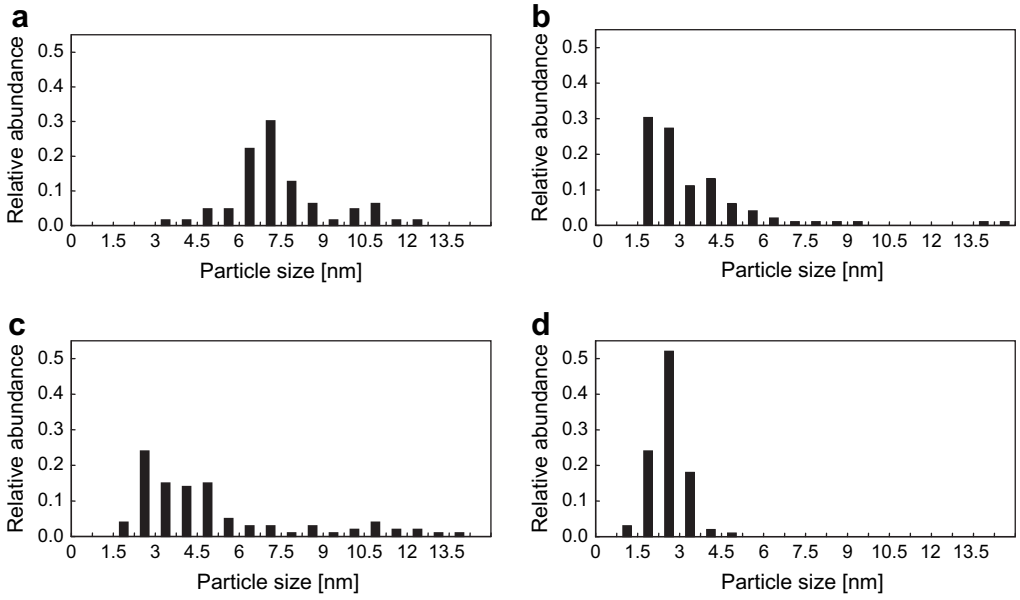

Fig. 5 – Histograms of particle size distribution for Pt catalyst particles supported on Vulcan XC-72: (a) Pt/VF; (b) Pt/VI; (c) Pt/VM, and (d) Pt/VC.

Other reduction methods employed to prepare Pt catalysts on carbon supports were included in Table 2 for comparison. The ethylene glycol [34] and colloidal [41] methods yield catalysts with particle sizes in the range of those prepared in this work, while the radiolytic [44] and ion exchange [32] methods lead to very small particles, although it should consider the differences in Pt loading of the studied catalysts.

3.2. *Dispersion and electrochemical active area*

In Table 3 the values of dispersion obtained from the hydrogen chemisorption isotherm are reported. The Pt/VF and Pt/VI catalysts exhibit better dispersion than the Pt/VM, although they all have lower dispersion values than the commercial catalyst (Pt/VC).

The average size of the Pt particles, d, can be obtained from the dispersion (N_S/N_T) resorting to the equations developed by van del Klink [45]:

$$N_T = \frac{2\pi}{3}\left(\frac{d}{a}\right)^3 \quad (2)$$

$$N_T = (10/3)l^3 - 5l^2 + (11/3)l - 1 \quad (3)$$

$$N_S = 10l^2 - 20l + 12 \quad (4)$$

where N_T is the total number of atoms, N_S the number of surface atoms, l the number of layers, and a is the lattice parameter, equal to 0.392 nm for Pt.

It can be observed in Table 3 that, while the dispersion values of the catalysts correlate with the particle sizes determined by TEM and XRD (except for Pt/VI, as mentioned above), the resulting average sizes obtained from the dispersion are significantly larger than those measured by TEM or XRD. The size of the Pt particles in the prepared catalysts are larger than that of the commercial one, although the sequence VM > VF ≈ VI > VC is not the same as that reported in Table 2 for the sizes determined by TEM or XRD. The difference in the average size of Pt particles determined by the different techniques could be due to an additional sinterization of Pt particles during the thermal H_2 pretreatment carried out before the chemisorption measurements. This process, taking into account the high-Pt-loading, would have different effect on the final particle size according to the reduction methods used in the preparation of the catalysts.

The initial rate for the cyclohexane dehydrogenation reaction (CDH) is also shown in Table 3. The Pt/VC catalyst has a higher dehydrogenation activity than the Pt/VF, Pt/VI and much higher than the Pt/VM catalyst. Taking into account that this reaction is not demanding or structure-insensitive [46], the dehydrogenation activity should increase with the exposed metal fraction, that is, the metal dispersion. It is observed from the results summarized in Table 3 that the expected correlation is obeyed and the decreasing sequence of CHD and Pt dispersion is Pt/VC > Pt/VF ≈ Pt/VI > Pt/VM.

The electrochemical active area (A_{EL}) of the catalysts reported in Table 3 was obtained from the charge required for hydrogen adsorption from the Pt surface, Q_H, calculated by integration of the adsorption peaks, as those shown in Fig. 6

Table 3 – Dispersion, electrochemical activity (A_{EL}), average Pt particle size determined from dispersion (d_D) and electrochemical activity (d_{AEL}), and activity in cyclohexane dehydrogenation of the Pt catalysts.

Catalysts	Dispersion (%)	d_D (nm)	A_{EL} ($m^2\ g^{-1}$)	d_{AEL} (nm)	CHD rate (mol CH/h g_{Pt})
VC (19.2%)	11.4	12	24	12	1.41
VF (20%)	8.1	16	21	13	0.91
VI (20%)	8.2	16	13	21	0.89
VM (20%)	5.6	24	20	14	0.41

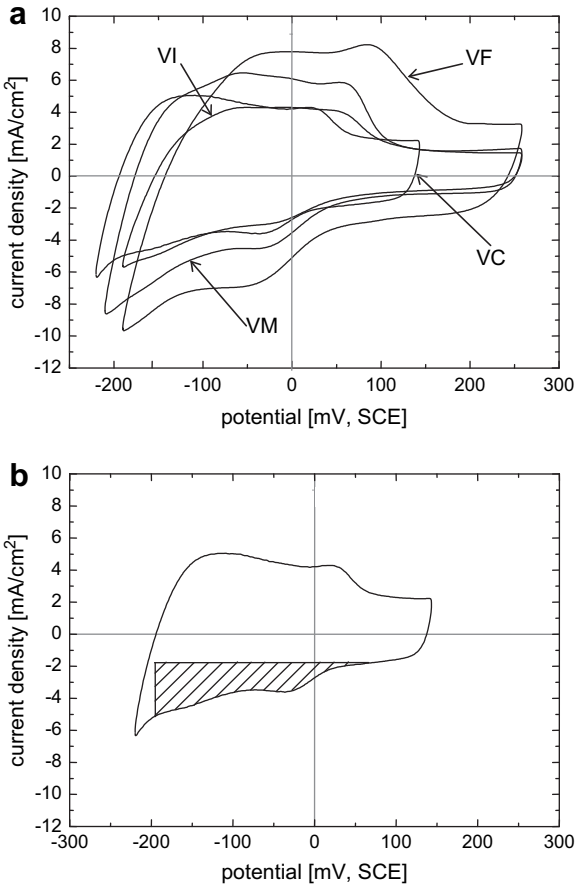

Fig. 6 – (a) Cyclic voltammetry on Pt catalysts supported on Vulcan carbon and prepared by different methods, in 1 M H_2SO_4 (scan rate 50 mV s^{-1}). Commercial catalyst Pt/VC was measured for comparison. (b) Example of one the cyclic voltammetry (VC) in which the integration area is shown (hatched area).

(the hatched region represents the integration area). The area was normalized with respect to the mass of platinum according to the equation:

$$A_{EL} = \frac{Q_H}{m_{Pt} Q_{Href}} \quad (5)$$

where Q_{Href} is a reference value equal to 0.21 mC cm^{-2} which arises from considering a surface density of 1.3×10^{15} atom-cm^{-2}, a generally adopted value for polycrystalline Pt [47], and m_{Pt} is the mass of platinum.

The average size of the particles can be obtained from A_{EL}, assuming uniform spherical particles, using the following equation [36]:

$$d = \frac{6}{\rho A_{EL}} \quad (6)$$

where $\rho = 21.4$ g cm^{-3} is the Pt density.

The results, summarized in Table 3, also lead to particle sizes larger than those measured by TEM and XRD, and are comparable with those calculated from dispersion, even when the sequence, VI > VM ≈ VF ≈ VC, is not the same. The different average particle sizes obtained from A_{EL} in comparison with those obtained from dispersion for the Pt/VF and Pt/VM catalysts would suggest that the coarsing process occurring during the chemisorption assay is more important for the Pt/VM catalyst, moderate for the Pt/VF, while it is absent for the commercial one.

It is interesting to compare the electrochemical active area of the E-TEK catalyst with the results reported in the literature [4,12,13,19,34–37,48,49] and is summarized in Fig. 7. As expected, A_{EL} decreases as the Pt loading increases, but a large data scatter is clearly observed, particularly at low-Pt-loading. Thus, the data for the Pt 20 wt% catalyst range from 28.6 $m^2 g^{-1}$ [49] up to 93 $m^2 g^{-1}$ [36], the former being close to the value measured in this work (see Table 3).

The observed scatter could be due, in part, to the integration area chosen to calculate Q_H, but more probably to the

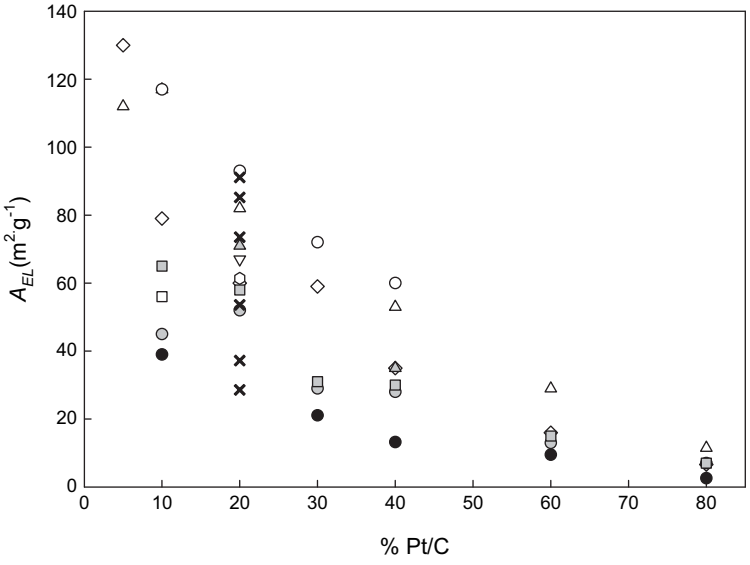

Fig. 7 – Electrochemical active area as a function of the catalyst Pt loading. Data from: (◇) Ref. [4]; (●) Ref. [12] in NaOH; (■) Ref. [12] in H_2SO_4; (●) Ref. [19]; (⌓) Ref. [34]; (△) Ref. [35]; (○) Ref. [36]; (▽) Ref. [37]; (□) Ref. [48]; (×) Ref. [49].

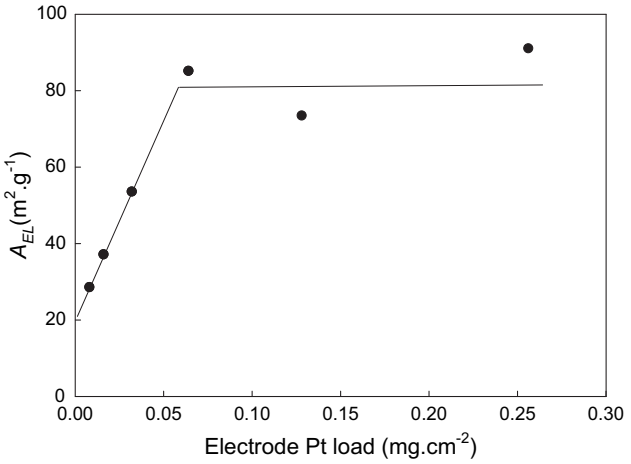

Fig. 8 – Electrochemical active area as a function of the electrode catalyst load. Data from Ref. [49].

effect of the thickness of the catalyst layer. Jiang and Yi [49] have recently shown that the electrochemical surface area of a 20 wt% Pt supported on Vulcan XC-72 increases with increasing catalyst layer thickness or, equivalently, the Pt loading of the electrode. Fig. 8 shows the behavior of the electrochemical active area with the Pt loading using the data reported in the literature [49]. It is observed that the electrochemical active area increases almost linearly with the Pt loading until a critical value (about 0.05 mg cm^{-2}). For higher Pt loading, the electrochemical active area seems to become insensitive to the thickness of the catalyst layer on the electrode. This increase of the Pt utilization, by a factor larger than three, with increasing catalyst thickness, was assigned to the hydrogen surface diffusion (spillover).

The measurements of the electrochemical active areas in this study were performed with thin catalyst layers and their A_{EL} values are expected to be lower than the ones reported in the literature using thicker electrodes. In spite of the fact that a detailed comparison is not possible because the thickness of the catalyst layer is not reported in most of the studies, the comparison of A_{EL} for our electrodes is meaningful because their thicknesses are similar.

According to the results shown in Table 3, the Pt/VF and Pt/VM catalysts exhibit high electrochemical activity, almost equal to the commercial one, while the value obtained for the Pt/VI is lower. A weak correlation is observed between A_{EL} and the dispersion, with the exception of the Pt/VI catalyst, which exhibits a low electrochemical active area in relation to its measured dispersion or average particle size. The presence of large Pt particles in the Pt/VI, catalyst, which accounts 25% of the exposed area, could explain the differences, having in mind that the electrochemical hydrogen sorption could depend on the crystallite structure of the platinum particles.

4. Conclusions

Nanoparticles of platinum catalysts were prepared on Vulcan XC-72 by three different chemical methods. The particle size of the catalysts was determined by TEM and XRD and compared to a commercial catalyst and to nanoparticulated platinum obtained by other method on several types of carbon supports. The average particles sizes of the prepared and commercial catalysts obtained by TEM technique are in good agreement with those obtained by XRD, except for Pt/VI catalyst in which the coexistence of small and large particles leads to different XRD and TEM averages. From the analysis of the abundant literature information on Pt particle size (Table 2), it is clear that TEM and XRD particle size values are rarely measured simultaneously, as performed in this work. The image that emerges from the comparison of our results and those reported in the literature is that, due to the heterogeneity of the samples, the average particle size obtained by the XRD technique, which scans the complete sample, are bigger and probably more representative of the macroscopic samples than TEM results. This is rather evident for the case of the catalyst prepared by the impregnation method (Pt/VI).

The Pt dispersion obtained by H_2 chemisorption on the prepared catalysts is lower than for the commercial (E-TEK) catalyst, particularly for the catalyst prepared by the microwave-assisted ethylene glycol method (Pt/VM). Although the CHD rate on the catalysts could not been quantitatively related with the Pt dispersion or particle size, the very good agreement with the dispersion obtained by H_2 chemisorption seems to indicate that the accessibility of H_2 to the catalyst surface is similar to that of the bulkier cyclohexane.

On the other hand, the Pt particle sizes obtained from the dispersion data are much larger than those measured by TEM and XRD, probably due that the additional H_2 treatment (before the isotherm determinations) produces a certain sintering of the metallic particles in a different magnitude according to the preparation method.

The Pt/VF and Pt/VM catalysts exhibit good electrochemical activity, similar to that observed for the commercial catalyst. The average Pt particle sizes obtained from the electrochemical activity does not seem to correlate with those determined from H_2 chemisorption, except for the commercial catalyst, but the low electrochemical activity of the Pt/VI catalyst could be related to the presence of large particles (bigger than 13 nm).

It is worthy to note that, in view of the big scatter observed in the literature for the values of A_{EL} obtained from catalyst layers with different thickness, a comparison of the A_{EL} only can be performed relative to catalysts with similar Pt loading on the support, as carried out in this work. Moreover, the relatively low values of A_{EL} obtained for all the catalysts in this study, as compared with values reported in the literature for 20 wt% Pt, obeys to the thin layer of catalyst (lower than 0.05 mg cm^{-2}) used in the preparation of the electrodes.

In summary, two of the three chemical methods analyzed here for the preparation of Vulcan Pt catalysts, the formic acid and the microwave-assisted ethylene glycol methods, seem to yield catalysts with low-Pt-loading and high-Pt-utilization. Other methods, such as electrodeposition, achieved the highest Pt utilization, but its application to large-scale manufacturing is doubtful due to concerns regarding its scalability [50]. On the other hand, the method of sputtering allows to deposit Pt directly onto the membrane electrolyte assembly (MEA) with ultra-low-Pt-loadings. However, the low

utilization and poor substrate adherence of the Pt remain challenges [50].

The chemical methods analyzed in this work do not require sophisticated set-up arrangements and since they are performed at low temperatures ($\leq$100 °C), both characteristics are attractive when thinking in large-scale production and low cost. Moreover, low temperature favors the productions of small particles with reasonably good size control by inhibiting the undesired processes of coarsening and coalescence.

Acknowledgments

The authors thank Griselda Polla and Miguel Torres for the experimental help and Fundación Antorchas for supporting the collaboration between INCAPE and CNEA groups. The financial support of ANPCyT (PICT SU 35403 and PAE 36985), CONICET (PIP 5977 and PIP 5431), and Universidad Nacional del Litoral (CAI + D) are gratefully acknowledged. F.J.N.P. thanks a doctoral fellowship from Consejo Nacional de Investigaciones Científicas y Técnicas (CONICET) and CNEA H.R.C. is member of CONICET.

REFERENCES

[1] Ticianelli EA, Berry JG, Srinivasan S. Dependence of performance of solid polymer electrolyte fuel cells with low platinum loading on morphologic characteristics of the electrodes. J Appl Electrochem 1991;21:597–605.
[2] Lee SJ, Mukerjee S, McBreen J, Rho YW, Kho YT, Lee TH. Effects of Nafion impregnation on performances of PEMFC electrodes. Electrochim Acta 1998;43:3693–701.
[3] Costamagna P, Srinivasan S. Quantum jumps in the PEMFC science and technology from the 1960s to the year 2000. Part I. Fundamental science aspects. J Power Sources 2001;102: 242–52.
[4] Stevens DA, Dahn JR. Electrochemical characterization of the active surface in carbon-supported platinum electrocatalysts for PEM fuel cells. J Electrochem Soc 2003;150:A770–5.
[5] Blurton KF, Greenburn P, Oswin HG, Rutt DR. The electrochemical activity of dispersed platinum. J Electrochem Soc 1972;119:559–64.
[6] Bett J, Lundquist J, Washington W, Stonehart P. Platinum crystallite size considerations for electrocatalytic oxygen reduction. Electrochim Acta 1973;18:343–8.
[7] Kinoshita K. Particle size effects for oxygen reduction on highly dispersed platinum in acid electrolytes. J Electrochem Soc 1990;137:845–8.
[8] Sattler ML, Ross PN. The surface structure of Pt crystallites supported on carbon black. Ultramicroscopy 1986;20:21–8.
[9] Peuckert M, Yoneda T, Dalla Betta RA, Boudart M. Oxygen reduction on small supported platinum particles. J Electrochem Soc 1986;133:944–7.
[10] Bregoli L. The influence of platinum crystallite size on the electrochemical reduction of oxygen in phosphoric acid. Electrochim Acta 1978;23:489–92.
[11] Watanabe M, Saegusa S, Stonehart P. Electro-catalytic activity on supported platinum crystallites for oxygen reduction in sulphuric acid. Chem Lett 1988;17:1487–90.
[12] Perez J, Gonzalez ER, Ticianelli EA. Oxygen electrocatalysts on thin porous coating rotating platinum electrodes. Electrochim Acta 1998;44:1329–39.
[13] Gasteiger HA, Kocha SS, Sompalli B, Wagner FT. Activity benchmarks and requirements for Pt, Pt-alloy, and non-Pt oxygen reduction catalysts for PEMFCs. Appl Catal B: Environ 2005;56:9–35.
[14] Thompsett D. Pt alloys as oxygen reduction catalysts. In: Vielstich W, Gaisteiger H, Lamm A, editors. Handbook of fuel cells – fundamentals, technology and applications, vol. 3. Chichester, UK: Wiley; 2003 [Chapter 37]p 467.
[15] Antoine O, Bultel Y, Durand R. Oxygen reduction reaction kinetics and mechanism on platinum nanoparticles inside Nafion. J Electroanal Chem 2001;(499)::85–94.
[16] Yano H, Inukai J, Uchida H, Watanabe M, Babu PK, Kobayashi T, et al. Particle-size effect of nanosclae platinum catalysts in oxygen reduction reaction: an electrochemical and ^{195}Pt EC-NMR study. Phys Chem Chem Phys 2006;8:4932–9.
[17] Takasu Y, Iwazaki T, Sugimoto W, Murakami Y. Size effects of platinum particles on the electro-oxidation of methanol in an aqueous solution of $HClO_4$. Electrochem Commun 2000;2:671–4.
[18] Park S, Xie Y, Weaver MJ. Electrocatalytic pathways on carbon-supported platinum nanoparticles: comparison of particle-size-dependent rates of methanol, formic acid, and formaldehyde electrooxidation. Langmuir 2002;18:5792–8.
[19] Bergamaski K, Pinheiro ALN, Teixeira-Neto E, Nart FC. Nanoparticle size effects on methanol electrochemical oxidation on carbon supported platinum catalysts. J Phys Chem B 2006;110:19271–9.
[20] Gonzalez ER, Ticianelli EA, Pinheiro ALN, Perez J. Processo de obtenção de catalisador de platina dispersa ancorada em substrato através da redução por ácido. Brazilean Patent INPI 003121; 1997.
[21] Lizcano-Valbuena WH, Paganin VA, Gonzalez ER. Methanol electro-oxidation on gas diffusion electrodes prepared with Pt–Ru/C catalysts. Electrochim Acta 2002;47:3715–22.
[22] de Miguel SR, Vilella JI, Jablonski EL, Scelza O, Salinas-Martínez de Lecea C, Linares-Solano A. Preparation of Pt catalysts supported on activated carbon felts (ACF). Appl. Catal. A: Gen. 2002;232:237–46.
[23] Liu Z, Gan LM, Hong L, Chen W, Lee JY. Carbon-supported Pt nanoparticles as catalysts for proton exchange membrane fuel cells. J Power Sources 2005;139:73–8.
[24] Zhang Y, Erkey C. Preparation of platinum–Nafion–carbon black nanocomposites via a supercritical fluid route as electrocatalysts for proton exchange membrane fuel cells. Ind Eng Chem Res 2005;44:5312–7.
[25] Zhang Y, Toebes ML, Van der Eerden A, ÓGrady WE, de Jong KP, Koningsberger DC. Metal particle size and structure of the metal-supported interface of carbon-supported platinum catalysts as determined with EXAFS spectroscopy. J Phys Chem B 2004;108:18509–19.
[26] Yasuda K, Nishimura Y. The deposition of ultrafine platinum particles on carbon black by surface ion exchange – increase in loading amount. Mater Chem Phys 2003;82:921–8.
[27] Coloma F, Sepúlveda-Escribano A, Fierro JLG, Rodriguez-Reinoso F. Preparation of platinum supported on pregraphitized carbon blacks. Langmuir 1994;10:750–5.
[28] Li W, Liang C, Qiu J, Zhou W, Han H, Wei Z, et al. Carbon nanotubes as support for cathode catalyst of a direct methanol fuel cell. Carbon 2002;40:787–803.
[29] Steigerwalt ES, Deluga GA, Lukehart CM. Pt–Ru/Carbon fiber nanocomposites: synthesis, characterization, and performances as anode catalysts of direct methanol fuel cells. A search for exceptional performance. J Phys Chem B 2002;106:760–6.
[30] Bessel CA, Laubernds K, Rodriguez NM, Baker RTK. Graphite nanofibers as an electrode for fuel cell applications. J Phys Chem B 2001;105:1115–8.
[31] Maillard F, Savinova ER, Simonov PA, Zaikovskii VI, Stimming U. Infrared spectroscopic study of CO adsorption

and electro-oxidation on carbon-supported Pt nanoparticles: interparticle versus intraparticle heterogeneity. J Phys Chem B 2004;108:17893–904.
[32] Gamez A, Richard D, Gallezot P. Oxygen reduction on well-defined platinum nanoparticles inside recast ionomer. Electrochim Acta 1996;41:307–14.
[33] Stevens DA, Zhang S, Chen Z, Dahn JR. On the determination of platinum particle size in carbon-supported platinum electrocatalysts for fuel cell applications. Carbon 2003;41: 2769–77.
[34] Yang R, Qiu X, Zhang H, Li J, Zhu W, Wang Z, et al. Monodispersed hard carbon spherules as a catalyst support for the electrooxidation of methanol. Carbon 2005;43:11–6.
[35] Geniès L, Faure R, Durand R. Electrochemical reduction of oxygen on platinum nanoparticles in alkaline media. Electrochim Acta 1998;44:1317–27.
[36] Maillard F, Martin M, Gloaguen F, Léger J-M. Oxygen electroreduction on carbon-supported platinum catalysts. Particle-size effect on the tolerance to methanol competition. Electrochim Acta 2002;47:3431–40.
[37] Paulus UA, Wokaun A, Scherer GG, Schmidt TJ, Stamenkovic V, Markovic NN, et al. Oxygen reduction on high surface area Pt-based alloy catalysts in comparison to well defined smooth bulk alloy electrodes. Electrochim Acta 2002;47:3787–98.
[38] See: <http://etek-inc.com/custom/product_C.php?prodid = 22#>.
[39] Jia N, Martin RB, Qi Z, Lefebvre MC, Pickup PG. Modification of carbon supported catalysts to improve performance in gas diffusion electrodes. Electrochim Acta 2001;46:2863–9.
[40] Smirnova A, Dong X, Hara H, Vasiliev A, Sammes N. Novel carbon aerogel-supported catalysts for PEM fuel cell application. Int J Hydrogen Energy 2005;30:149–58.
[41] Gharibi H, Mirzaie RA, Shams E, Zhiani M, Khairmand M. Preparation of platinum electrocatalysts using carbon supports for oxygen reduction at a gas-diffusion electrode. J Power Sources 2005;139:61–6.
[42] Elezović NR, Babić BM, Hrstajić NV, Gajić-Krstajić LM, Vračar LjM. Specificity of the UPD of H to the structure of highly dispersed Pt on carbon support. Int J Hydrogen Energy 2007;32:1991–8.
[43] Grigoriev SA, Lyutikova EK, Martemianov S, Fateev VN. On the possibility of replacement of Pt by Pd in a hydrogen electrode of PEM fuel cells. Int J Hydrogen Energy 2007;32: 4438–42.
[44] Legratiet B, Remita H, Picq G, Delcourt MO. CO-stabilized supported Pt catalysts for fuel cells: radiolytic synthesis. J Catal 1996;164:36–43.
[45] van der Klink JJ. NMR spectroscopy as a probe of surfaces of supported metal catalysts. Adv Catal 2000;44:1–117.
[46] Blankey DW, Somorjai GA. The dehydrogenation and hydrogenolysis of cyclohexane and cyclohexene on stepped (high miller index) platinum surfaces. J Catal 1976; 42:181–96.
[47] Biegler T, Rand DAJ, Woods R. Limiting oxygen coverage on platinized platinum; relevance to determination of real platinum area by hydrogen adsorption. J Electroanal Chem 1971;29:269–77.
[48] Marie J, Berthon-Fabry S, Achard P, Chatenet M, Pradourat A, Chainet E. Highly dispersed platinum on carbon aerogels as supported catalysts for PEM fuel cell-electrodes: comparison of two different synthesis paths. J Non-Cryst Solids 2004;350: 88–96.
[49] Jiang J, Yi B. Thickness effects of a carbon-supported platinum catalyst layer on the electrochemical reduction of oxygen in sulfuric acid solution. J Electroanal Chem 2005;577: 107–15.
[50] Wee J-H, Lee K-Y, Kim SH. Fabrication methods for low-Pt-loading electrocatalysts in proton exchange membrane fuel cell systems. J Power Sources 2007;165:667–77.